Dalton Transactions

Accepted Manuscript

ROYAL SOCIETY OF CHEMISTRY

www.rsc.org/dalton

Effects of the electronic structure of five-membered N-heterocyclic carbenes on insertion of silanes and boranes into the NHC C-N bond

Kalon J. Iversen, David J. D. Wilson and Jason L. Dutton**

Department of Chemistry, La Trobe Institute for Molecular Science, La Trobe University, Melbourne, Victoria, Australia, 3086

ABSTRACT

The effect of varying the N-heterocyclic carbene (NHC) ligand on the ring expansion and endocyclic C-N activation of NHCs by silanes and boranes has been investigated with theoretical methods. Five common NHCs were considered, including unsaturated, saturated, 3,4-methyl, 3,4-chloro substituted five-membered NHCs and a fused benzimidazole NHC. The substrates considered were Ph_2SiH_2 (with two hydrides migrating to the carbene carbon), H_2BMe (two hydrides migrating), $HBMe_2$ (hydride migration, followed by methyl migration) and BMe_3 (two methyls migrating). Consistent with experimental observations, it was found that the kinetic barrier is lowest for the saturated NHC. The barrier is also quite low for the benzimidazole NHC. It was determined that the partial positive charge on the central carbene carbon in the initial adduct is inversely proportional to the magnitude of the activation barrier.

INTRODUCTION

Recently, experimental and theoretical studies have described activation of the C-N bond of N-heterocyclic carbenes (NHCs) by element hydrides, alkyls and aryls (equations 1-7, Scheme 1).[1] Despite NHCs being considered to be a robust spectator ligand in catalysis, the activation of C-N bonds has significant generality, being thus far observed for the elements Be,[2] B,[3-5] Si,[6] Ni,[7] and Zn.[8] In the case of Zn and B, ring expansion was observed during catalytic reactions, indicating that this class of transformation should be considered as a potential decomposition pathway in catalysis using NHC containing complexes.

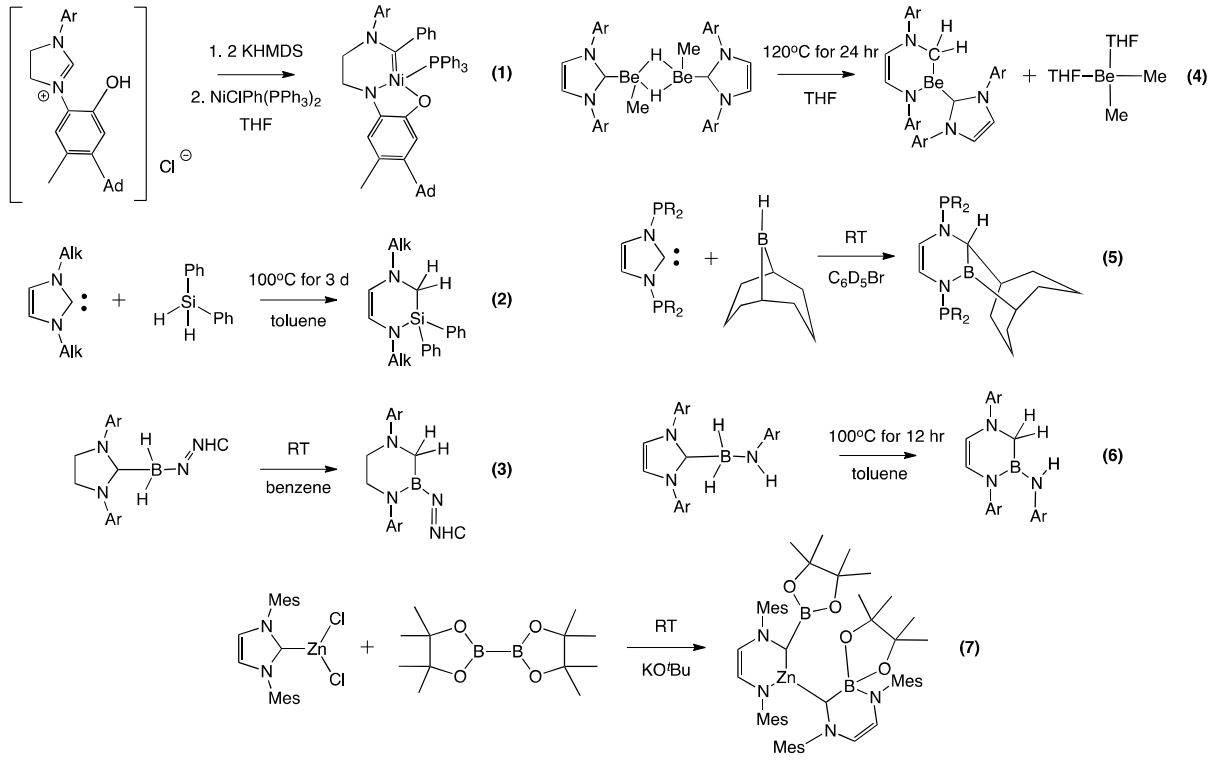

Scheme 1. Representative reactions involving insertion of an inorganic element into the C-N bond of N-heterocyclic carbenes (NHCs).

The mechanism for ring expansion, originally postulated by Radius[6] for silane insertion, and later validated by several theoretical studies for Be, B, and Si insertion,[9-13] involves four distinct steps (illustrated in Scheme 2):

1. Formation of an NHC-element hydride adduct (A)
2. Migration of a hydride (or alkyl/aryl group) from the element to the carbenic carbon (B).
3. Insertion of the element hydride into the ring C-N bond (C).
4. Migration of the second hydride (or alkyl/aryl group) to the carbenic carbon giving the final product (D).

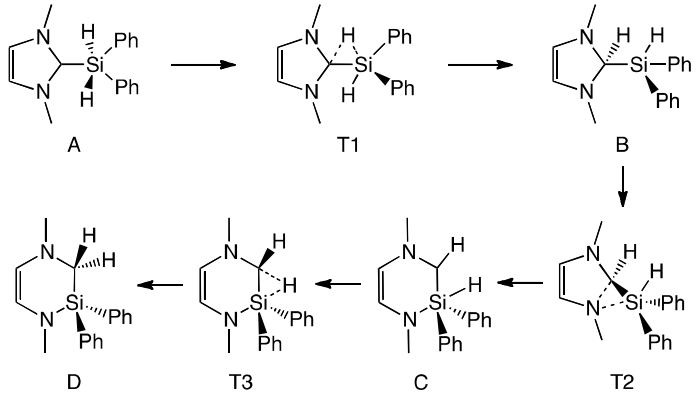

Scheme 2. Calculated reaction pathway for ring expansion via C-N bond activation, using Ph_2SiH_2 as the substrate.

Theoretical studies of B, Be and Si hydride insertion found that in each case the rate-determining step is the initial hydride migration.[9-13] The barrier height for T1 (hydride migration) was calculated to range from 55 to 120 kJ/mol, which is consistent with experimental studies that required elevated temperatures (80-150 ^{o}C) and extended reaction times (typically longer than 24 hours).[1] Migration of H at both T1 and T3 was found to be more favorable than migration of an aryl group or a halide, although aryl migration at T3 has been observed experimentally.

Experimental studies suggest that ring insertion occurs under milder conditions when a saturated NHC is used.[5,6] Thus far, theoretical studies with NHCs have almost exclusively focused on

unsaturated NHCs with the standard structure **1** (Figure 1). The exception is the study of Rivard and Brown that considered borane insertion into a cyclic alkylaminocarbene (cAAC), which showed that for cAAC the C-N bond activation is not feasible due to a large barrier for the C-N bond insertion (T2).[11] The same study also considered NHC **5** (amongst some more exotic fused ring NHCs) in the reaction with Ph_2SiH_2, which as discussed below in the context of the results presented here, has negligible differences with NHC **1** for this substrate. Su considered main group NHC analogues with C-Pb at the N-E-N position, and found that reactivity towards ring expansion decreases in going down the group.[9]

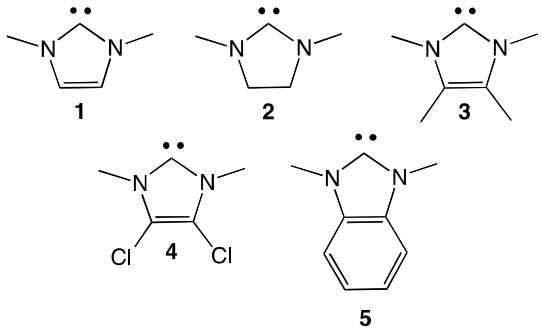

Figure 1. N-heterocyclic ligands considered in this work.

Here we report the results of a theoretical investigation into the effect of the NHC electronic on the relative thermodynamic energies and kinetic barriers for ring insertion. The NHCs considered in this study are illustrated in Figure 1 (**1**-**5**), which were chosen to represent a cross-section of the five-membered NHCs typically used in synthetic studies. N-heterocyclic carbene **1** is a model of the most common "Arduengo" type unsaturated NHC, while **2** is the saturated analogue. N-Heterocyclic carbene **3** is a model of a common modification of the unsaturated NHC with methyl groups at the 3 and 4 position of the ring; **4** contains electron-withdrawing chlorine substituents, and **5** is a model of the frequently used benzimidazole NHC. For computational efficiency, only methyl groups were considered as the N-substituent on each NHC.

The model insertion element species chosen for this study were boranes (BMe_3, $BHMe_2$, BH_2Me) and silanes (Ph_2SiH_2). These were chosen, since the experimental reaction pathways are the most well-defined for elements that undergo the insertion reaction (for Be and Zn the starting complex is not definitively known).

RESULTS AND DISCUSSION

Silane

The first reaction considered was the insertion/migration reaction of Ph_2SiH_2 into NHCs **1-5** with the transfer of two hydrides. Plots of the free energy reaction profiles are given in Figure 2, with calculated thermochemical values presented in Table 1. As calculated previously, the reaction proceeds via an initial (experimentally unobserved) adduct that is higher in energy than the starting materials by 57-73 kJ/mol. The T1 barrier (defined relative to the NHC and silane starting materials) for **1** and **3-5** are similar, ranging from 120 to 132 kJ/mol (51-71 kJ/mol above A); the saturated NHC (**2**) gives a lower barrier at 95 kJ/mol (28 kJ/mol above A). Indeed, for **2** the barrier to Si insertion in the ring C-N bond (T2) is actually higher than T1, being 154 kJ/mol. The prediction that T2 is the rate-determining step for **2** is consistent with experimental observations from the groups of Bertrand and Radius on the reaction of this carbene (with 2,6-diisopropylphenyl N-substituents) with $PhSiH_3$.[6,14] For reactions at room temperature, their isolated products were analogous to compound B, and only upon heating to 100 °C did conversion to compound D occur (Scheme 3). For the reaction of **5** with Ph_2SiH_2, insertion of Si into the C-N bond (T2) is also predicted to be the rate-determining step (T1 120 kJ/mol; T2 145 kJ/mol). The T1 barrier is similar to that of **1** (127 kJ/mol), which suggests that elevated temperatures would likely be required to overcome the T1 barrier for **5** and thus isolation of compound B would likely be difficult to achieve for **5**.

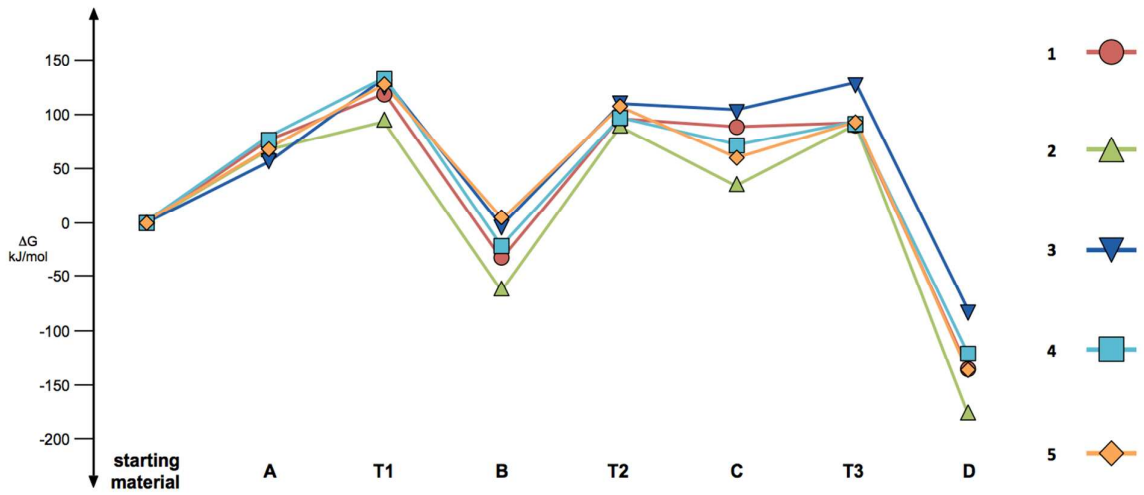

Figure 2. SCS-MP2/def2-TZVP calculated reaction profile (ΔG_{298K}, kJ/mol) for hydride migration/ring expansion of NHCs **1-5** with Ph_2SiH_2 as the substrate.

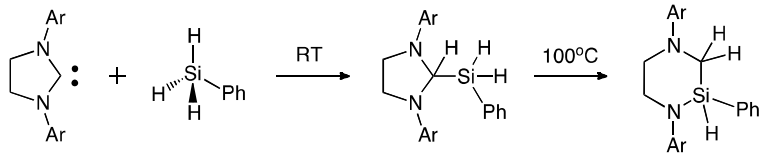

Scheme 3. Reported reactions of H_3SiPh with NHC **2** (with 2,6-diisopropyl N-substituents (Ar) in the synthetic report).

Table 1. SCS-MP2/def2-TZVP calculated reaction pathways for hydride migration and ring insertion of NHCs **1-5** (ΔG, kJ/mol).

		Reaction coordinate energy, ΔG (kJ/mol)						
Insertion compound	NHC compound	A	T1	B	T2	C	T3	D
	1	66.1	127.2	-0.5	107.2	57.0	90.9	-126.6
	2	66.5	94.6	-63.7	89.8	31.9	89.8	-180.0
Ph_2SiH_2	3	56.7	128.1	-6.3	109.1	100.5	128.4	-89.8
	4	72.7	131.6	-23.7	93.0	66.8	87.7	-137.4
	5	69.3	119.9	-37.3	107.7	85.2	87.5	-138.7
	1	-129.8	15.4	-39.1	-24.1	-111.7	-63.9	-208.4
	2	-134.4	-44.5	-99.2	-72.0	-112.2	-105.4	-267.6
H_2BMe	3	-139.3	16.8	-45.1	-22.8	-74.1	-28.1	-172.4
	4	-120.4	8.6	-51.9	-37.3	-106.0	-63.0	-206.8
	5	-131.3	-14.4	-61.7	-40.7	-98.4	-74.4	-224.1
	1	-95.8	38.1	-3.5	-7.0	-92.5	-21.4	-162.5
	2	-96.9	-23.4	-78.9	-49.1	-93.6	-64.9	-211.5
$HBMe_2$	3	-105.1	44.6	-6.2	-3.8	-55.0	16.3	-127.3
	4	-86.9	45.6	-27.5	-20.9	-80.3	-20.3	-166.5
	5	-92.6	12.8	-37.2	-25.8	-81.0	-34.2	-182.0
	1	-54.8	113.0	23.7	34.5	-52.8	24.9	-112.2
	2	-54.1	59.5	-32.4	-5.6	-60.8	-21.1	-166.4
BMe_3	3	-57.3	115.9	19.3	35.3	-10.6	65.4	-75.5
	4	-40.9	111.9	10.4	18.4	-44.5	20.3	-113.9
	5	-47.6	77.6	-12.3	14.2	-38.9	12.1	-126.6

The barrier for the second hydride migration (T3) is quite low for the unsaturated NHCs, ranging from 2 kJ/mol (**5**) to 34 kJ/mol (**1**). For **2** the barrier is 58 kJ/mol, and although larger, it is still only about half that of the respective T1 barrier (95 kJ/mol). Thermodynamically, the overall reaction involving **2** is most favourable, with ΔG about 40 kJ/mol more negative than that for **1**, **4** and **5** and 90 kJ/mol more favourable than **3**.

The difference in the T1 barrier and overall reaction Δ*G* between saturated **2** and unsaturated **1**, **3**-**5** may be understood in terms of the electronic structure of the NHC. Since hydride migration and ring insertion of the silane results in a loss of aromatic character for the ring, it is instructive to consider the aromaticity of **1**-**5**, for which nucleus independent chemical shift (NICS) values have been calculated (Table 2). The values for NHC **1** are in agreement with previous results.[15,16] A negative NICS value is indicative of aromaticity, a positive NICS value indicates anti-aromatic character and values around 0 ppm are consistent with non-aromatic rings.[17] Since saturated **2** already possesses non-aromatic character, it does not need to overcome the same extent of disruption to ring aromaticity as does **1**, **3**-**5** as a result of hydride migration and ring expansion. This is consistent with the T1 barrier being lower for **2**, and subsequently Δ*G* for the overall reaction being most favourable with **2**.

Table 2. MP2/def2-TZVP calculated NICS values (ppm) for **1**-**5**. [a]

NHC	NICS(0)	NICS(1)	$NICS(1)_{zz}$
1	-12.6	-10.1	-28.8
2	-4.9	-3.0	-3.3
3	-11.6	-9.8	-26.6
4	-12.5	-9.3	-24.4
5	-10.5	-10.0	-25.2

[a] NICS(0) is the isotropic shielding calculated at the centre of the ring, NICS(1) is calculated 1 Å above the ring centre, and $NICS(1)_{zz}$ is the out-of-plane component of shielding calculated 1 Å above the ring plane.

Boranes

The next substrates considered in this study were three boranes with varying numbers of methyl substituents: H_2BMe, $HBMe_2$ and BMe_3. The three reactions were modeled to compare the transfer of two hydrides (H_2BMe), one hydride and one methyl ($HBMe_2$) and two methyl groups (BMe_3). Calculated results are presented in Table 1. The primary difference between the reaction profile of the silane and the boranes is that for the boranes, formation of the initial adduct (A) between the NHC and the borane is thermodynamically favourable. Adduct formation is most favourable for H_2BMe (Δ*G* of -120 to -140 kJ/mol), followed by $HBMe_2$ (Δ*G* of -85 to -105 kJ/mol) and finally

BMe_3 (ΔG of -40 to -57 kJ/mol). In each case, NHC **4** forms the least stable adduct while **3** forms the most stable adduct.

For H_2BMe (Figure 3), the T1 barrier (calculated relative to compound A) is calculated to be lowest for saturated **2** (90 kJ/mol), which is analogous to the silane case. For **5** the T1 barrier is 117 kJ/mol, while for **1**, **3** and **4** the barriers are 129-156 kJ/mol. For each NHC, the T2 barrier (insertion of boron into the ring C-N bond, 15-27 kJ/mol) is much lower than that of T1, which suggests that isolation of compound B is unlikely for this class of substrate with five-membered NHCs. The barrier for the second hydride migration (T3) is also lower than that of T1, and so C→D is also not competitive as the rate-determining step for any of the NHCs. The T3 barrier for **2** is only 7 kJ/mol, while for **5** it is 24 kJ/mol and for **1**, **3**-**4** it is 43-48 kJ/mol. In fact, for **1**, **3**-**5** the T3 barrier is actually lower than that of T2. Hence, if sufficient energy were available to overcome the rate-determining T1 barrier, then product D would be readily produced. For the overall reaction, insertion into **2** is the most thermodynamically favourable, which is analogous to the silane case.

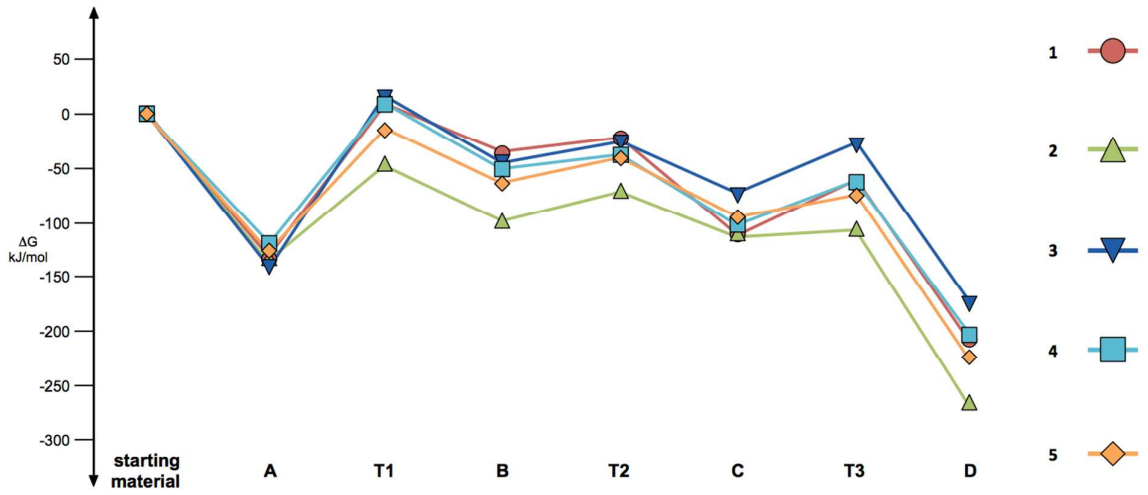

Figure 3. SCS-MP2/def2-TZVP calculated reaction profile (ΔG_{298K}, kJ/mol) for hydride migration/ring expansion of NHCs **1**-**5** with H_2BMe as the substrate.

For $HBMe_2$, where ring insertion requires migration of at least one methyl group to the carbenic carbon, it is found that the favoured pathway involves initial hydride migration (T1) followed by

ring expansion (T2) and a final methyl migration (T3). Initial migration of the methyl was considered, however the barrier at T1 for methyl migration is calculated to be much higher than for migration of the hydride. The preference for hydride migration has been consistently predicted by theoretical studies,[9-13] and also observed experimentally.[5,6]

Trends in the T1 barriers (H migration) for $HBMe_2$ are similar to that of Ph_2SiH_2 and H_2BMe, being lowest for **2** (74 kJ/mol) and **5** (105 kJ/mol), with the other three NHCs having higher barriers of 132 to 150 kJ/mol. The T2 barrier is again negligible for **1**, **3**-**5** (all below 12 kJ/mol), and while for **2** the barrier of 30 kJ/mol is larger, it is still less than half that of T1. In all cases the T3 barrier for methyl migration (29-71 kJ/mol) is significantly smaller than the T1 barrier, being approximately half that of the corresponding T1 barrier. Compound **2** is again distinctly different, being the only NHC for which the T2 barrier is greater than that of T3. For the overall reaction, insertion into **2** is the most thermodynamically favourable, which is analogous to the silane and H_2BMe cases.

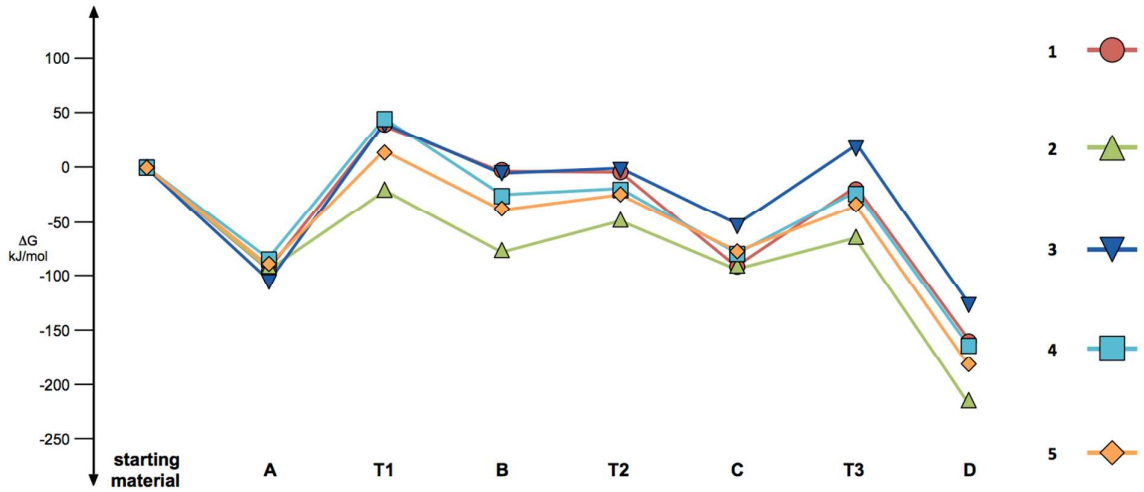

Figure 4. SCS-MP2/def2-TZVP calculated reaction profile (ΔG_{298K}, kJ/mol) for hydride/alkyl migration/ring expansion of NHCs **1**-**5** with $HBMe_2$ as the substrate.

For BMe_3, the first methyl migration step at T1 is rate determining in all cases. The T1 barrier is again lowest for **2** (114 kJ/mol), followed by **5** (125 kJ/mol) and **1**, **3**-**4** (153-173 kJ/mol). These barriers would imply that significant heating would be required to drive each reaction over T1. In comparison, the T2 barriers are negligible, while T3 is less than half that of T1 in each case. Hence the final steps are not a significant factor with respect to the overall predicted rates (compared to T1). Again, the overall reaction is most favourable for **2** (ΔG = -166 kJ/mol).

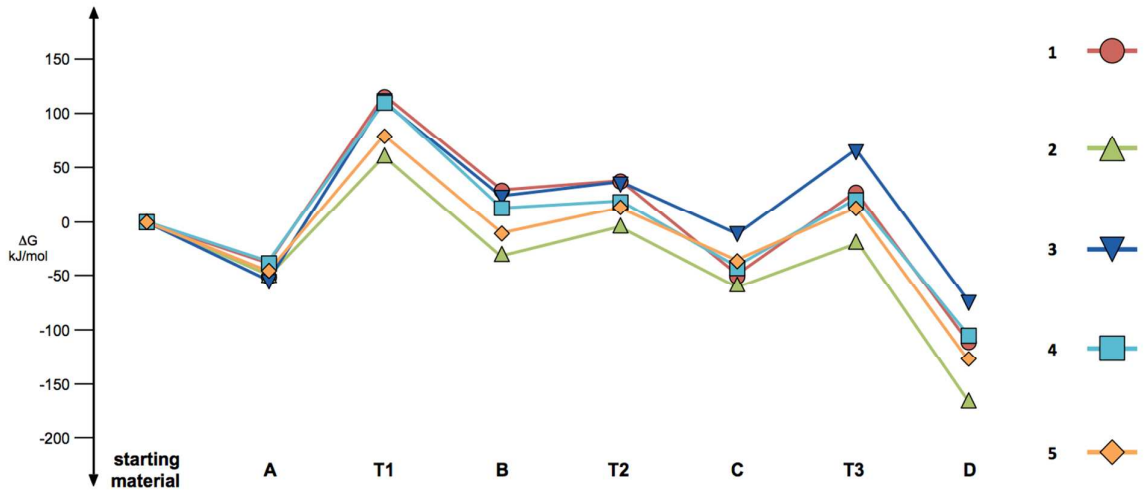

Figure 5. SCS-MP2/def2-TZVP calculated reaction profile (ΔG_{298K}, kJ/mol) for hydride/alkyl migration/ring expansion of NHCs **1**-**5** with BMe_3 as the substrate.

Comparison of the three boranes produces several trends worth noting. Firstly, the overall reaction is always most favourable with **2**, which also has the lowest T1 barriers. The methyl-substituted NHC (**3**) yields the highest T1 barrier and smallest magnitude of overall reaction free energy. In all cases, formation of T1 is the rate-determining step. For **2**, the T2 barrier is largely independent of the borane, being 27-30 kJ/mol (moreover, for Ph_2SiH_2 it is 28 kJ/mol). In contrast, the T3 barrier for **2** is clearly influenced by the number of borane methyl groups, which successively increase the T3 barrier. For example, with H_2BMe the T3 barrier is 7 kJ/mol, while with $HBMe_2$ it is 29 kJ/mol, and for BMe_3 the T3 barrier is 40 kJ/mol.

The lower T1 barrier for **2** may be rationalized by reference to the non-aromatic nature of the starting NHC, in the same manner as for the silane insertion. However, for the three borane cases the T1 barrier with **5** is substantially lower than that for **1**, **3** and **4**, making arguments based exclusively on aromaticity somewhat unsatisfying. The NICS values in Table 2 do not suggest that there is any noticeable distinction between the aromatic character of **5** and **1**, **3**-**4**.

The electronic stability of the transition state at T1 was further evaluated by comparing B3LYP/def2-TZVP calculated HOMO-LUMO (H-L) gaps for the T1 transition-state complexes (Table 3). For all borane substrates, **2** exhibits the largest H-L gap. However, a comparison of H-L gaps and activation energies for the other NHCs indicates that these properties are poorly correlated.

Table 3. B3LYP/def2-TZVP calculated HOMO-LUMO gaps (eV) for T1 transition state complexes.

	Borane substrate		
NHC	H_2BMe	$HBMe_2$	BMe_3
1	4.23	5.21	4.91
2	5.67	6.44	6.25
3	4.11	4.81	4.72
4	4.61	5.26	5.07
5	4.37	4.83	4.84

We then hypothesized that if the migration of the hydride/methyl group is based on a nucleophilic attack of the fragment onto the carbenic carbon, the relative Lewis acidity or electrophilicity of the carbon in adduct A may be a better indicator of reactivity. Natural bond orbital (NBO) charges for the carbene carbon of A were calculated (Supporting Information, Table S1), whereby a partial positive charge was used as an indication of the capacity of this carbon to accept the hydride or methyl group. For all substrates a good correlation is obtained between the barrier from A to T1 and the partial charge (Figure 6), with **2** and **5** having the most positive charge on the carbon atom, coupled with the lowest activation barriers. NHC **3** is the largest outlier, with slightly larger activation barriers than **1** despite having slightly lower charges on the carbon in adduct A, but overall the correlation appears reasonable.

The correlation between the NBO charge on the carbene carbon and the propensity for hydride migration suggests that this might be a useful tool for predicting the stability of adducts. The reliability of the correlation was investigated by consideration of the basis set (def2-SVP, def2-TZVP) and functional dependence (B3LYP, M06-2X, M06-L, BP86 and B3LYP-D3BJ). Results are collated in Table S2 in the Supplementary Information. In general, most correlations (r^2) are above 0.8, and are marginally greater using ΔE_e rather than ΔG. The lowest values of r^2 are above 0.5. Basis set effects are mostly minimal, with r^2 varying by less than 0.08 between def2-SVP and def2-TZVP for all functionals except B3LYP, for which the mean absolute deviation (MAD) between def2-SVP and def2-TZVP is 0.16, which is dominated by large deviations for $BHMe_2$ and BMe_3. M06-2X yielded the largest average r^2 values with both basis sets (>0.92), closely followed by BP86 (>0.85) and M06-L (>0.84). It is suggested that the M06-2X/def2-TZVP approach is ideal for predicting the stability of adducts.

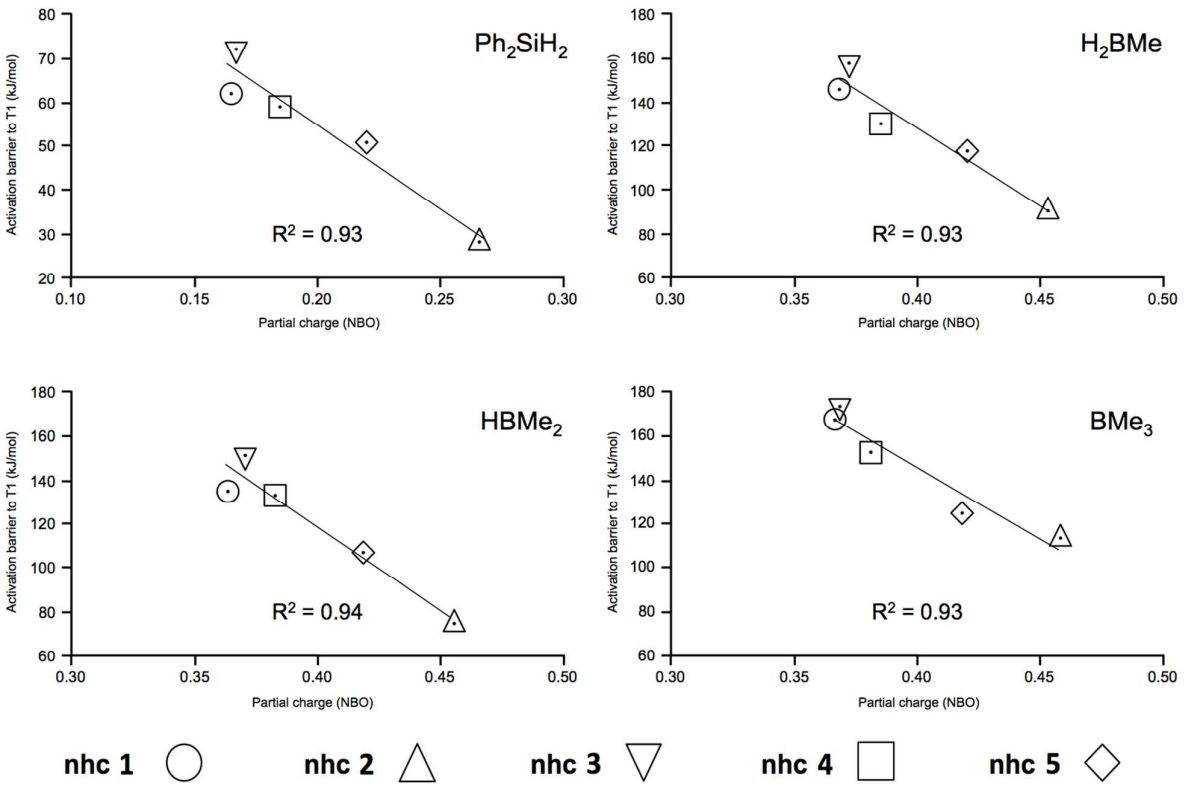

Figure 6. Plots of B3LYP/def2-TZVP calculated NBO partial charges on the carbenic carbon against activation barrier (difference between adduct A and transition state T1).

The partial positive charge on the carbene carbon is related to the π-accepting properties of carbenes. Recently Bertrand and co-workers demonstrated that the π-accepting capacity of a variety of carbenes could be related to the ^{31}P NMR chemical shifts of phosphinidine adducts (i.e. NHC-P-Ph).[18] A more downfield ^{31}P NMR chemical shift is indicative of greater π-accepting capability for a given carbene. As this is an experimentally measurable value, we investigated the correlation between the activation barrier at T1 and the ^{31}P NMR chemical shifts determined for the NHC-P-Ph adducts for the four NHCs (**1**-**3**, **5**) considered both in Bertrand's study and ours (Figure 6). For **1** and **2**, Bertrand used aryl N-substitutents rather than the methyl N-substituents considered here, however it was noted in the experimental study that changing the steric arrangement of the aryl group (2,6-diisopropylphenyl vs mesityl) only had a subtle effect on ^{31}P chemical shifts. It is hypothesized that the difference in N-substituent will not significantly impact the relationship

between ^{31}P chemical shift and the activation barrier, which are plotted in Figure 7. There is a good correlation ($R^2 > 0.87$) between the activation barrier for the insertion/ring expansion reaction and the ^{31}P NMR chemical shift of the NHC-P-Ph adducts for all four of the main group substrates considered here.

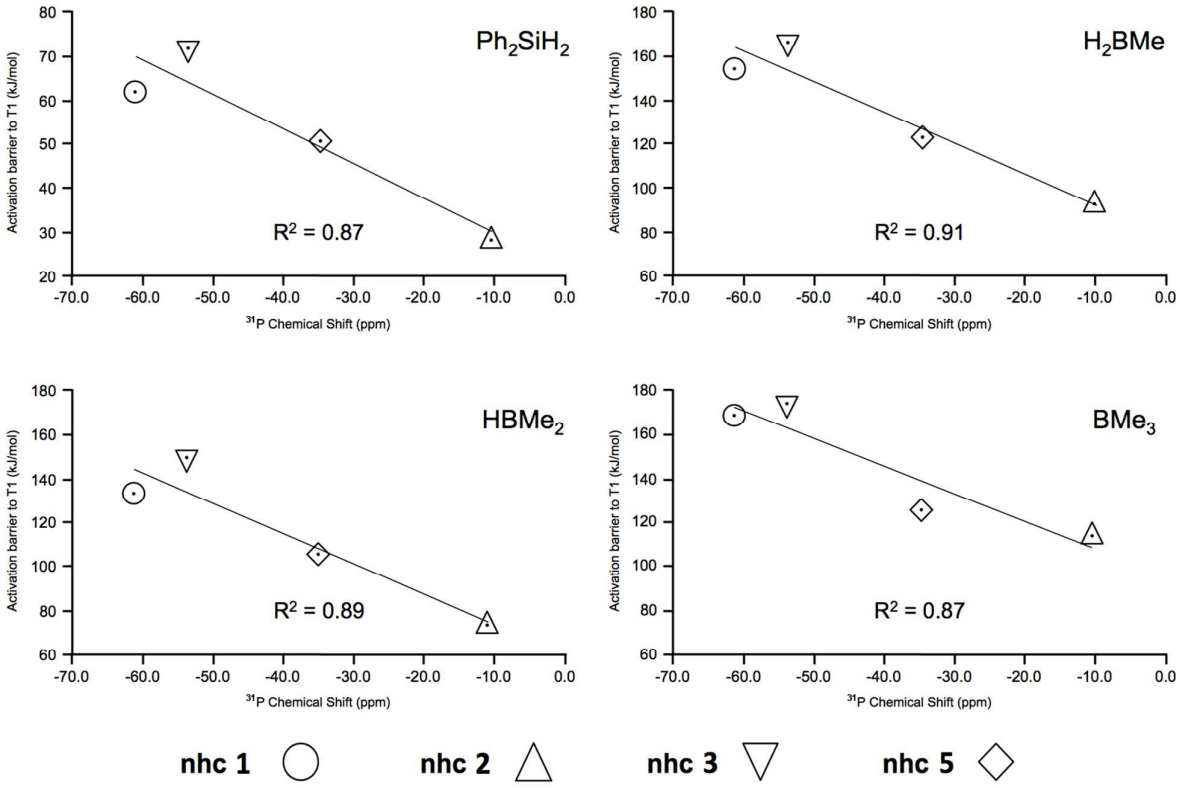

Figure 7. Activation barrier at T1 plotted against the experimentally determined ^{31}P NMR chemical shifts of phosphinidine (NHC-P-Ph) adducts of NHCs **1**, **2**, **3** and **5**.

CONCLUSIONS

A computational investigation of the effect of NHC environment on E-H(R) mediated ring insertion has been carried out, for which it is concluded that the class of five-membered NHC has a significant effect on the kinetics (reaction barriers) of the insertion/ring expansion reaction. Consistent with experimental observations, the barrier for the initial H migration (T1) is lowest for

the saturated NHC (**2**), with T2 (E-R insertion into the NHC C-N bond) becoming rate determining for silane substrates. Larger differences in the barrier for the various NHCs are observed for borane substrates, with fused benzimidazole NHC (**5**) also having a distinctly lowered barrier. A reasonable inverse correlation was found between the barrier at T1 and the partial charge on the central carbon in adduct A, allowing for the inference that the electrophilicity of the carbon in adduct A is the key factor in determining the barrier. The M06-2X/def2-TZVP method is recommended for the prediction of adducts that may undergo hydride migration. We hope this study may act as a guide for synthetic chemists in selecting NHCs to study this class of reaction, or in selecting NHCs in cases where they may want to avoid the ring expansion when combining NHCs with susceptible substrates.

COMPUTATIONAL DETAILS

All theoretical calculations were performed using the Gaussian 09 program.[19] Geometry optimisations were carried out using the M06-2X density functional[20] and def2-TZVP basis set.[21] Frequency calculations, performed at the same theory level, indicated that all optimised structures were minima on the potential energy surface. Transition state optimisations used the quadratic synchronous transit (QST) method.[22] All transition states were also confirmed using intrinsic reaction coordinate (IRC)[23] analysis. Thermodynamic corrections for energy values were taken from these calculations (standard T = 298.15 K and p = 1 atm). Geometry optimisations were also performed using other density functionals (B3LYP[24,25] and PBE[26]) and basis sets (6-31G(d)[27,28] and def2-SVP[29]), all of which produced comparable geometries. Single-point energies were calculated at the M06-2X/def2-TZVP geometries, including MP2, SOS-MP2[30] and SCS-MP2[31] energies. Additional single-point energies were calculated with M06-2X, M06-L, BP86 and B3LYP-D3BJ. All reported ΔG values are SCS-MP2 electronic energies with M06-2X/def2-TZVP thermochemical corrections. Molecular orbital (MO) analysis was carried out at the B3LYP/def2-TZVP level of

theory at the M06-2X optimized geometries, as the results provided good agreement with previous studies. NBO analysis was carried out with NBO 5.9.[32]

ASSOCIATED CONTENT

Supporting Information. Cartesian coordinates and energies for optimized geometries. This material is available free of charge via the Internet at http://pubs.acs.org.

AUTHOR INFORMATION

Corresponding Author

*david.wilson@latrobe.edu.au, j.dutton@latrobe.edu.au

ACKNOWLEDGMENT

We thank The La Trobe Institute for Molecular Science for their generous funding of this project. Grants of computing resources from VPAC and NCI-NF are acknowledged. This work is also supported by an ARC DECRA fellowship (JLD, DE130100186).

REFERENCES

(1) Iversen, K. J.; Wilson, D. J. D.; Dutton, J. L. *Dalton Trans.* **2014**, *43*, 12820.
(2) Arrowsmith, M.; Hill, M. S.; Kociok-Köhn, G.; MacDougall, D. J.; Mahon, M. F. *Angew. Chem. Int. Ed.* **2012**, *51*, 2098.
(3) Al-Rafia, S. M. I.; McDonald, R.; Ferguson, M. J.; Rivard, E. *Chem. Eur. J.* **2012**, *18*, 13810.
(4) Wang, T.; Stephan, D. W. *Chem. Eur. J.* **2014**, *20*, 3036.
(5) Franz, D.; Inoue, S. *Chem. Asian. J.* **2014**, *9*, 2083.
(6) Schmidt, D.; Berthel, J. H. J.; Pietsch, S.; Radius, U. *Angew. Chem. Int. Ed.* **2012**, *51*, 8881.
(7) Waltman, A. W.; Ritter, T.; Grubbs, R. H. *Organometallics* **2006**, *25*, 4238.
(8) Bose, S. K.; Fucke, K.; Liu, L.; Steel, P. G.; Marder, T. B. *Angew. Chem. Int. Ed.* **2014**, *53*, 1799.
(9) Su, M.-D. *Inorg. Chem.* **2014**, *53*, 5080.
(10) Fang, R.; Yang, L.; Wang, Q. *Organometallics* **2014**, *33*, 53.
(11) Momeni, M. R.; Rivard, E.; Brown, A. *Organometallics* **2013**, *32*, 6201.
(12) Iversen, K. J.; Wilson, D. J. D.; Dutton, J. L. *Dalton Trans.* **2013**, *42*, 11035.
(13) Iversen, K. J.; Wilson, D. J. D.; Dutton, J. L. *Organometallics* **2013**, *32*, 6209.
(14) Frey, G. D.; Masuda, J. D.; Donnadieu, B.; Bertrand, G. *Angew. Chem. Int. Ed.* **2010**, *49*, 9444.
(15) Guna, A. K.; Sarmah, S.; Phukan, A. K. *Dalton Trans.* **2010**, *39*, 7374.

(16) Rojisha, V. C.; De, S.; Parameswaran, P. *Inorg. Chem.* **2012**, *51*, 8265.
(17) Schleyer, P. v. R.; Maerker, C.; Dransfeld, A.; Jiao, H.; van Eikerma Hommes, N. J. R. *J. Am. Chem. Soc.* **1996**, *118*, 6317.
(18) Back, O.; Henry-Ellinger, M.; Martin, C. D.; Martin, D.; Bertrand, G. *Angew. Chem. Int. Ed.* **2013**, *52*, 2939.
(19) Frisch, M. J.; Trucks, G. W.; Schlegel, H. B.; Scuseria, G. E.; Robb, M. A.; Cheeseman, J. R.; Scalmani, G.; Barone, V.; Mennucci, B.; Petersson, G. A.; Nakatsuji, H.; Caricato, M.; Li, X.; Hratchian, H. P.; Izmaylov, A. F.; Bloino, J.; Zheng, G.; Sonnenberg, J. L.; Hada, M.; Ehara, M.; Toyota, K.; Fukuda, R.; Hasegawa, J.; Ishida, M.; Nakajima, T.; Honda, Y.; Kitao, O.; Nakai, H.; Vreven, T.; J. A. Montgomery, J.; Peralta, J. E.; Ogliaro, F.; Bearpark, M.; Heyd, J. J.; Brothers, E.; Kudin, K. N.; Staroverov, V. N.; Kobayashi, R.; Normand, J.; Raghavachari, K.; Rendell, A.; Burant, J. C.; Iyengar, S. S.; Tomasi, J.; Cossi, M.; Rega, N.; Millam, J. M.; Klene, M.; Knox, J. E.; Cross, J. B.; Bakken, V.; Adamo, C.; Jaramillo, J.; Gomperts, R.; Stratmann, R. E.; Yazyev, O.; Austin, A. J.; Cammi, R.; Pomelli, C.; Ochterski, J. W.; Martin, R. L.; Morokuma, K.; Zakrzewski, V. G.; Voth, G. A.; Salvador, P.; Dannenberg, J. J.; Dapprich, S.; Daniels, A. D.; Farkas, Ö.; Foresman, J. B.; Ortiz, J. V.; Cioslowski, J.; Fox, D. J.; Revision D.1; Gaussian, Inc.: Wallingford CT, 2009.
(20) Zhao, Y.; Truhlar, D. G. *Theor Chem Account* **2008**, *120*, 215.
(21) Schäfer, A.; Huber, C.; Ahlrichs, R. *The Journal of Chemical Physics* **1994**, *100*, 5829.
(22) Peng, C.; Ayala, P. Y.; Schlegel, H. B.; Frisch, M. J. *Journal of Computational Chemistry* **1996**, *17*, 49.
(23) Fukui, K. *Accounts of Chemical Research* **1981**, *14*, 363.
(24) Becke, A. D. *Physical Review A* **1988**, *38*, 3098.
(25) Lee, C.; Yang, W.; Parr, R. G. *Physical Review B* **1988**, *37*, 785.
(26) Ernzerhof, M.; Perdew, J. P. *The Journal of Chemical Physics* **1998**, *109*, 3313.
(27) Hehre, W. J.; Ditchfield, R.; Pople, J. A. *The Journal of Chemical Physics* **1972**, *56*, 2257.
(28) Hariharan, P. C.; Pople, J. A. *Theoretica chimica acta* **1973**, *28*, 213.
(29) Schäfer, A.; Horn, H.; Ahlrichs, R. *The Journal of Chemical Physics* **1992**, *97*, 2571.
(30) Jung, Y.; Lochan, R. C.; Dutoi, A. D.; Head-Gordon, M. *The Journal of Chemical Physics* **2004**, *121*, 9793.
(31) Grimme, S. *The Journal of Chemical Physics* **2003**, *118*, 9095.
(32) E. D. Glendening; J. K. Badenhoop; A. E. Reed; J. E. Carpenter; J. A. Bohmann; C. M. Morales; Weinhold, F.; NBO 5.9. see http://www.chem.wisc.edu/~nbo5: Theoretical Chemistry Institute, University of Wisconsin, Madison, WI, 2011.